Histochemistry (1995) 103:135–145

ORIGINAL PAPER

Michael Rickmann · Joachim R. Wolff

Modifications of S100-protein immunoreactivity in rat brain induced by tissue preparation

Accepted: 17 October 1994

Abstract Immunocytochemistry using antibodies against various molecular forms of the Ca^{++} and Zn^{++}-binding S100 proteins predominantly labelled astrocytes. However, especially in the neocortex the staining pattern is variable. Methods of tissue preparation have been evaluated with the aim to preserve as much S100 immunoreactivity as possible. Optimal results were obtained after perfusion fixation with 4–5% aldehydes, 0.1 *M* sodium cacodylate, 0.1% $CaCl_2$, pH 7.3. In such preparations, astrocytes were completely labelled including their lamellar compartments in large parts of the central nervous system. Ca^{++}-withdrawal had adverse affects on S100 immunoreactivity. Cryostat sections treated with EDTA-containing solutions before fixation showed that Ca^{++}-free S100 can apparently not be fixed to the tissue. Perfusion fixatives containing EDTA resulted in inhomogeneous loss of S100 staining, indicating a differential susceptibility of astrocytic subpopulations. A different type of reduction in S100 immunoreactivity occurred around large neocortical blood vessels. Perivascular defects in immunostaining occasionally appeared even after optimal fixation, but could be regularly provoked by mildly acidic fixation (pH 6.6) or prolonged barbiturate anaesthesia. These defects might be based on S100 release into the cerebrospinal fluid. Presumably under none of the conditions studied can the immunoreactivity of all S100-forms and -fractions be completely preserved in the tissue. However, recommendations are presented for optimizing tissue preparation, to the extent that premortal modifications affecting the stainability of astrocytes may be detected by S100 immunohistochemistry in fixed brain tissue.

Introduction

In the mammalian brain, the Ca^{2+}- and Zn^{2+}-binding S100 proteins (S100) occur at high concentrations (1–1.5 µg/mg of soluble protein; Matsutani et al. 1985). Applying immunohistochemical methods to tissues fixed with aldehydes, the bulk of S100 has been localized in cell bodies, processes and lamellae of astrocytes (e.g. Matus and Mughal 1975; Cocchia 1981; Tabuchi et al. 1983). Colocalization with glial fibrillary acidic protein (GFAP) confirmed the astroglial location of S100 (Boyes et al. 1986). Therefore, it is generally assumed that S100 is predominantly localized in glial cells (Moore 1988), especially in astrocytes, although there are also reports on the localization of this antigen in oligodendrocytes (Ludwin et al. 1976; Dyck et al. 1993) and even in neurons (Goto et al. 1988, see below).

S100 proteins have several biochemical properties which may influence or distort their immunohistochemical detectability. The relatively small molecular size (~21 kDa) make these proteins highly soluble in the cytosol, i.e. S100 is predominantly found in "non-particulate" subcellular fractions (for review see Moore 1988). Membrane-bound S100 may amount to more than 10% of the total (Donato et al. 1986; Donato 1991), but this percentage may vary with the functional state of the neuropil (Popov et al. 1988). Changes in S100 binding may be based on the binding of Ca^{2+}- or Zn^{2+}-ions to S100, which induces changes in the conformation, sulphhydryl reactivity and hydrophobic properties of S100 (Baudier et al. 1986; Baudier and Cole 1988). Furthermore, S100 proteins can differ in their subunit composition from α- and β-chains. From brain tissue, mainly the dimeric forms S100b ($\beta\beta$) and S100a ($\alpha\beta$) were isolated. The relative amounts of S100b and S100a show high interspecies variation, e.g. the rat brain contains more than 95% S100b (Kato et al. 1990).

In addition, there are reports on the artificial displacement of S100 in immunocytochemical preparations. Early findings of S100 immunoreactivity in certain neurons could have been caused by inadequate fixation (Rapport et al. 1974) and/or diffusion of astroglial S100 as discussed by Ghandour et al. (1981). Artificial displacement of S100 can apparently be avoided by perfusion fixation (Eng and Bigbee 1978). Since translocation of

M. Rickmann (✉) · J.R. Wolff
Zentrum Anatomie, Kreuzbergring 36,
D-37075 Göttingen, Germany

S100 can also occur in vivo, it is important to avoid such technical pitfalls. Intravitally, S100 may be released into the extracellular space of the central nervous system under various physiological and pathological conditions. This suggestion is suppported by high concentrations of S100 found in the cerebrospinal fluid (CSF) of rats (Shashoua et al. 1984; Hårdemark et al. 1989). In the CSF of human control individuals, S100 concentrations range between <1 and 6.8 ng/ml but may rise up to 700 ng/ml under pathological conditions (Persson et al. 1987).

When searching for sites of artificial or physiological release of S100, the large number of submicroscopic lamellar extensions of astrocytes have to be taken into account. These lamellae contain S100 (Cocchia 1981), are thinner than 0.3 µm and have to be analysed under the electron microscope (Wolff 1965). In the neocortex, astroglial lamellae constitute about 50% of the total astroglial cell volume (Wolff 1968; Rohlmann et al. unpublished results).

S100 immunohistochemistry may detect functionally relevant patterns of S100 distribution in astrocytes of certain brain regions, an aspect that seems especially important for the neocortex and hippocampus. In these brain regions, effects of S100 on neuroplasticity have been shown (Lewis and Teyler 1986; Müller et al. 1993), which in turn may influence S100 immunoreactivity of astrocytes (Haring et al. 1993). A special role for S100 in the cerebral cortex is also documented by the increase of S100b in aging rats (Kato et al. 1990). Recently, we presented preliminary evidence that patterns of S100 immunoreactivity may vary between different regions of the forebrain and that premortal conditions may modify these distribution patterns of S100 immunoreactivity (Rickmann and Wolff 1992; Laskawi et al. 1993).

Thus, a combination of premortal and artificial factors may interfere with S100 immunohistochemistry and obscure important functional aspects of the distribution of S100 in brain tissue. Here, we investigate in detail ways in which S100 immunoreactivity may be influenced by anaesthesia and the composition of fixatives. Two aims were followed especially for the rat cerebral cortex. On the one hand, we tried to optimize the tissue preparation technique in order to maximize S100 immunoreactivity. On the other hand, we investigated influences of specific suboptimal conditions on the preservation of S100 immunoreactivity in brain tissue, especially the neocortex of rats.

Materials and methods

Animals, anaesthesia

Adult Sprague-Dawley rats ranging from 60 to 180 days of age were kept at normal diurnal rhythm of 12 h and had access to food and water ad libitum. Most animals (38 rats) were deeply anaesthetized with ether prior to perfusion fixation and/or removal of brain tissue. A total of 13 rats were anaesthetized by different means. For CO_2-anaesthesia (2 rats) animals were kept in a glass container filled with a mixture of CO_2 and air until the respiratory rhythm changed (less than 2 min). Other narcotics were injected intraperitoneally: Ketavet/Rompun were applied to 3 rats as a mixture of 113.7 mg ketamine hydrochloride and 9.2 mg 2,6-dihydro-2-(2,6-xylidino)-4H-1,3-thiazine hydrochloride per kg body weight. A total of 6 rats were injected with 1.25 g/kg urethane. Pentobarbital anaesthesia lasting for 1 h and carried out on 2 rats was initiated by an injection of 30 mg/kg and maintained by a second injection of 24 mg/kg 30 min later.

Tissue preparation

Transcardial perfusion fixation was performed at a hydrostatic pressure of 1 m water column. The vascular system was flushed with a buffer solution until the jugular veins had cleared (about 2 min). Subsequently a fixing solution was infused (10 min at room temperature) containing the same buffer and ionic additives as the rinsing solution. For postfixation, brains were removed from the skull and submerged for various periods of time in the same fixative that was used for perfusion. Unfixed brains were rapidly removed from the skull and frozen in melting isopentane within less than 2 min after respiratory arrest. For immersion fixation small pieces of tissue <3 mm in diameter were submerged in fixative at room temperature.

Fixatives, buffer, pH, additives

The composition of various types of aldehyde-containing fixatives was as follows: (1) 4% paraformaldehyde and 0.1% $CaCl_2$ in 0.1 *M* sodium cacodylate at pH 7.3 with addition of 0 to 1% glutaraldehyde. (2) The relative amounts of these aldehydes were reversed (1.5% paraformaldehyde and 2.5% glutaraldehyde). (3) Different buffers (0.1 *M* sodium phosphate and 0.1 *M* sodium/potassium phosphate, 80 m*M* Na^+/20 m*M* K^+) both at pH 7.3 were mixed with 4% paraformaldehyde, 0.3% glutaraldehyde. (4) For trapping of divalent cations the respective fixative was buffered by 0.1 *M* sodium cacodylate containing 10 mM EDTA. Two different versions of periodate-lysine-paraformaldehyde fixative were used. An acidic solution was mixed according to the original recipe (McLean and Nakane 1974). Alternatively, paraformaldehyde was added to the lysine-phosphate buffer until a final concentration of 4% was reached, and the pH was readjusted to 7.3. Sodium metaperiodate was added immediately before use.

Precipitation of S100 in ammonium sulphate was combined with aldehyde fixation by treating cryostat sections with a saturated solution of ammonium sulphate containing 4% paraformaldehyde at pH 3.7. Glutaraldehyde could not be mixed with ammonium sulphate, because solutions turned yellow indicating instability of this aldehyde. For carbodiimide fixation a 2% solution of 1-ethyl-3(3-dimethylaminopropyl)-carbodiimide hydrochloride (EDPC, Sigma) was prepared in 0.1 *M* sodium phosphate buffer at pH 7.3 (Turner 1972; Kendall et al. 1971).

Vapour fixation

Cryostat sections of 15 µm in thickness were dried overnight at −20° C in a desiccator containing silica gel. Sections were then transferred to vials containing diethylpyrocarbonate (DEPC) or 1,2-benzoquinone dissolved in toluene (Pearse and Polak 1975) or dry paraformaldehyde. The containers were tightly closed and heated to 60° C for 1 h. After rehydration, free floating sections were processed for immunocytochemistry.

Freeze substitution

Brain pieces of 2 mm in thickness were impact frozen on the polished surface of a copper block cooled by liquid nitrogen (Verna 1983). Then the tissue was substituted and chemically fixed in 1% glutaraldehyde dissolved in 98% acetone at −40° C for 4 days, before being rehydrated at room temperature and subjected to immunocytochemistry.

Sections

Cryostat sections of unfixed brain were mounted on slides of which the surfaces were activated by the following pretreatment. Cleaned microscope slides were incubated in sealed containers containing 10% γ-aminopropyl-triethoxysilane (Weetall 1970) in toluene overnight at room temperature. After washing in toluence and acetone they were air dried and reacted in 1% glutaraldehyde in water for 6 h, thoroughly rinsed in water and dried again. Sections were attached to the surface of these slides so firmly that they could be kept moist up to the transfer into buffer or fixing solutions. The bulk of material examined in this study consisted of a series of sections of 50 µm in thickness cut from fixed brain. Fixed tissue blocks were either sectioned on a vibratome under 50 m*M* TRIS, 150 m*M* NaCl, pH 7.6 (TBS) or soaked overnight in 20% sucrose and cut on a freezing microtome.

Immunohistochemistry

Immunocytochemical demonstration of S100 was performed with the avidin-biotin-peroxidase complex (ABC) method (Hsu et al. 1981). A rabbit antiserum against S100 (Dako) was used at dilutions of 1:1000 or 1:2000, the optimal range of dilution determined in a test series. Ascites fluid containing monoclonal G12B8-antibodies (Haan et al. 1982) kindly provided by these authors was diluted 1:1000. For negative controls either normal rabbit serum or control ascites were used at appropriate concentrations. For positive controls, immunocytochemistry of GFAP (rabbit antiserum, Dako) or vimentin (monoclonal antibodies, Dako) was applied to sections of the same series. Sections were processed at room temperature through the following incubation steps: (1) Two to four hours incubation in blocking solution containing 0.1 *M* DL-lysine, 1% bovine serum albumin (BSA), 1:10 normal goat serum, 0.02% sodium azide in TBS. (2) Primary antibodies diluted in blocking solution for 12 h. (3) Rinsing three times for 20 min in TBS. (4) Secondary antibodies for 1 h; biotinylated goat-anti-rabbit or goat-anti-mouse antibodies (Dako) were diluted 1:500 in blocking solution. (5) Three further rinses in TBS, 20 min each. (6) ABC-complex for 1 h; the complex was mixed from 1:250 biotinylated peroxidase an 1:250 streptavidin in 1% BSA in TBS for 45 min before use. (7) Three rinses in TBS and one rinse in 0.1 *M* sodium phosphate, pH 7.2, for 20 min each. (8) Histochemical visualization of peroxidase using diaminobenzidine hydrochloride (DAB) and Ni/Co-intensification according to Adams (1981). The reaction mixture consisted of 0.025% DAB, 0.025% $CoCl_2$, 0.02% $(NH_2SO_3)_2Ni{\cdot}xH_2O$, 0.01% H_2O_2 in 0.1 *M* sodium phosphate, pH 7.2, and was applied for 10 min. (9) Four rinses in 0.1 *M* sodium phosphate at pH 7.2 for 5 min each.

For light microscopy, the stained vibratome or frozen sections of 50 µm in thickness were soaked in 0.5% gelatin in 40% ethanol, mounted on microscope slides and air dried at 37° C for 1–3 days. Dehydration through a graded ethanol series (starting with 70%) and xylene was followed by coverslipping in Entellan (Merck). Stained cryostat sections already mounted on slides were kept moist and dehydrated through a complete ethanol series and xylene before coverslipping.

For electron microscopy the same immunohistochemical protocol was used as described above. Subsequently, vibratome sections were treated with 2% OsO_4 in 0.1 *M* sodium phosphate, pH 7.2, for 1 h followed by two rinses in the same buffer. After dehydration through a graded ethanol series and propylene oxide they were infiltrated with Spurr's low-viscosity embedding medium and placed on microscope slides. To obtain flat embedding of sections, several of these slides were piled on tops of each other being separated by 1-mm-thick polypropylene sheaths, clamped together and polymerized at 70° C for 24 h. Selected sections were polymerized to the flat surface of an epoxy block and detached from the slide. Sections were cut of 2 µm in thickness and examined in the light microscope. Semithin sections showing optimal penetration by the immunological reagents were selected for resectioning. Ultrathin sections wre stained with uranyl acetate (25 min) followed by lead citrate (3 min) (Venable and Coggeshall 1965) or bismuth oxynitrate (1 min; Riva 1974).

Results

In neocortical tissue, most of the S100 immunoreactivity was found in astrocytes, and astroglial staining defects were the most sensitive indicator of suboptimal conditions during tissue preparation. Figure 1 shows the staining patterns obtained in various brain regions by immunohistochemistry with antibodies against S100. The present analysis was focused on the neocortex, where astrocytic S100 immunoreactivity was relatively high but appeared sensitive to the various conditions applied. Comparisons of different methods of tissue preparation were based on observations of corresponding cortical areas and laminae.

Optimal conditions for S100 immunoreactivity

The protocol leading to the most complete immunostaining for S100 is as follows. The vascular system was rinsed by transcardial perfusion with 0.1% $CaCl_2$ in 0.1 *M* sodium cacodylate buffer (pH 7.3) followed by a fixative containing 4% paraformaldehyde, 0.3% glutaraldehyde in the same buffer (10 min). Postfixation of the

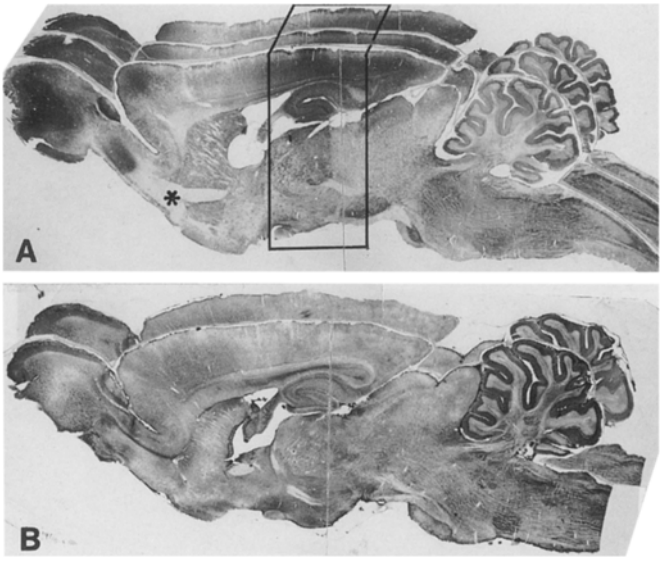

Fig. 1. A, B Similarity of S100-immunoreactivity patterns among serial parasagittal sections from adult rat brains fixed by perfusion with 4% paraformaldehyde, 0.5% glutaraldehyde in 0.1 *M* sodium phosphate, pH 7.3. **A** frozen sections of 50 µm in thickness. Note the low staining intensity of the anterior commissure (*asterisk*) and some other, but not all, parts of white matter. **B** Vibratome sections of 50 µm show reduced immunoreactivity in some but not all brain regions. Reduced immunoreactivity in frontal cortex of (**A**) and high immunoreactivity in the cerebellum of (**B**) are apparently individual variations confirmed in adjacent sections. ×2.9. Electron microscopic analysis was restricted to the *framed* block of tissue

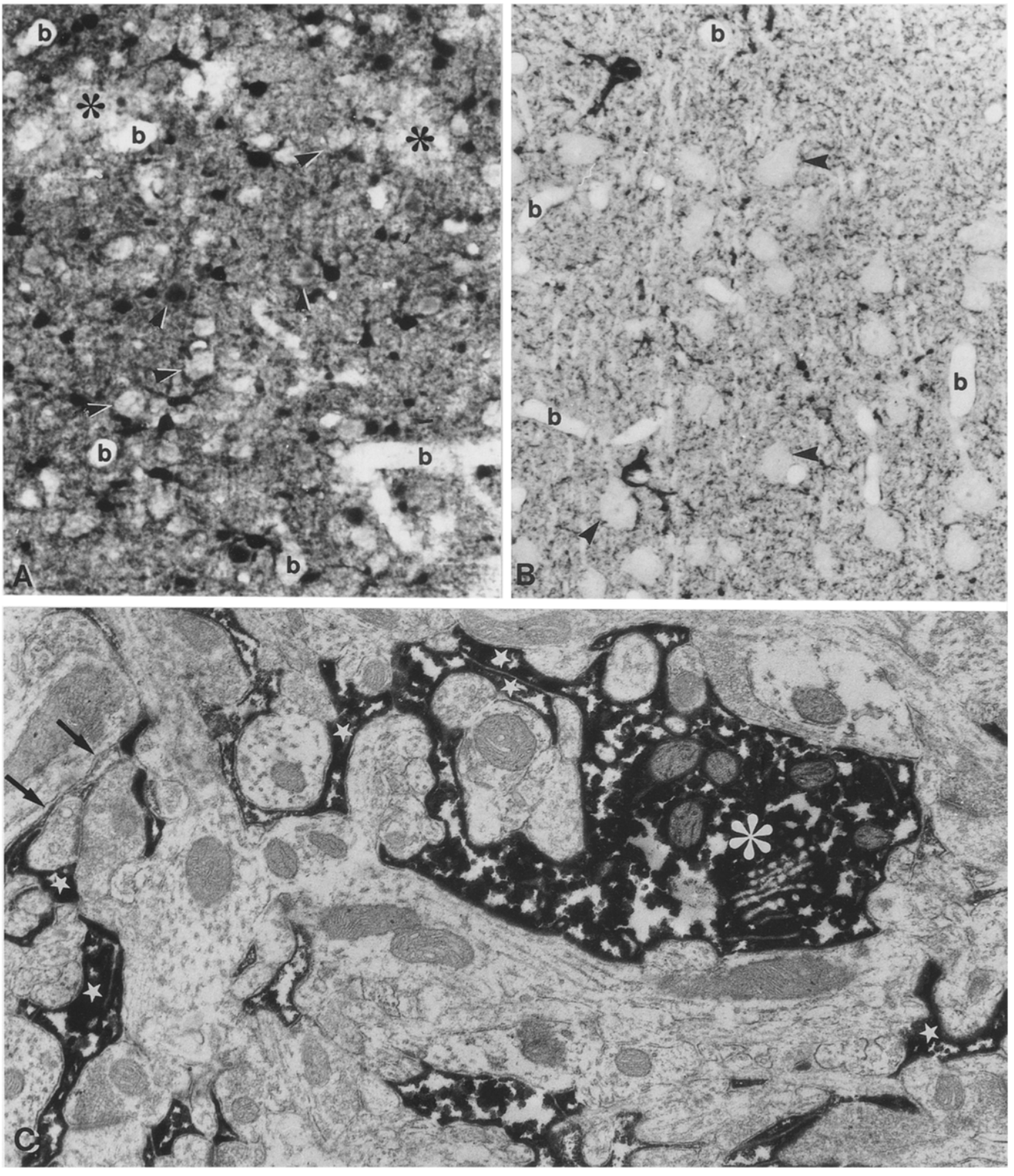

Fig.2 A–C Comprehensive labelling of astrocytes with S100 antibodies applied to the neocortex of adult rat. **A** Vibratome section of 40 μm treated with detergent (Triton X100) shows superimposition of many labelled processes of astrocytes. Small zones with lighter staining (*asterisks*) either indicate underlying neuronal perikarya, which are unstained, or selective loss of S100 immunoreactivity from small processes of tangentially cut astrocytes. Note that neuronal cell nuclei are mostly unstained, but a few show S100 staining at variable density (cf. *arrowheads*). **B** In a semithin section, immunostained astroglial processes can be seen throughout the neuropil but no staining is seen over neuronal cell bodies (*arrowheads*). Medium sized blood vessels are labeled 'b'. **C** Ultrathin section cut parallel to the surface of a vibratome section shows an astroglial process (*asterisk*) and almost complete labelling of astroglial lamellae (*stars*). In some lamellae thinner than 50 nm little reaction product is found (*arrows*). **A** ×550; **B** ×875; **C** ×22700

whole brain was done in the same fixative for 2 h. In the following, all variations of tissue preparation will be described in relation to this procedure of "standard fixation".

Under these conditions, the DAB-reaction product was almost evenly distributed in astrocytes including the cytosol of cell bodies, processes and lamellar extensions. The geometry of these cells had to be considered when the completeness of S100 labelling was analysed. Cell bodies and processes are studded with innumerable submicroscopic lamellae. Specialized parts of astrocytes are those processes and lamellae which form sheaths beneath the meningeal surfaces and around blood vessels where they are often extremely thin (<0.1 μm). Because astroglial processes and lamellae permeate the neuropil at high density, frozen sections or detergent treated vibratome sections of 40 μm in thickness tended to be completely opaque. Cell bodies and major processes could be delineated but smaller processes and lamellae disappeared within a diffuse background staining (Fig. 2A). S100-labelled processes were clearly seen in semithin sections cut from the very surface of vibratome sections. Even in 2-μm-thick sections there was background staining due to astrocytic lamellae which cannot be resolved at the level of the light microscope (Fig. 2B).

Electron microscopy revealed that astroglial lamellae completely filled with reaction product after standard fixation were restricted to a zone near to the surface of vibratome sections (Fig. 2C). In lamellar portions thinner than 50 nm the reaction product became faint, probably of restricted penetration of antibodies (arrows in Fig. 2C). Although the overall immunoreactivity of the polyclonal antiserum was higher than that of the monoclonal G12B8 antibody after standard fixation, the specificity and structural completeness of astrocytic labelling of both antibodies were identical at the structural level.

The effects of tissue preparation on S100 preservation in astrocytes was studied mainly with the polyclonal antiserum and in vibratome sections that were not permeabilized by freezing or detergents. In these sections, immunological reagents and the DAB-reaction product penetrated to a maximum depth of approximately 5 μm, while complete lamellar staining was restricted to the outer 2 μm, when checked by electron microscopy. Thus, cell bodies and the majority of processes could be observed by light microscopy. The distribution of S100 labelling in submicroscopic astroglial processes had to be estimated from the contrast between zones of greyish staining and unstained structures such as empty blood vessels, endothelial cells and most neurons (Fig. 2B).

Also in optimally treated preparations, S100 immunoreactivity may be reduced or even lost from restricted zones of cortical tissue. Such defects were especially seen in the neuropil neighbouring some large intracortical blood vessels (asterisks in Fig. 2A). A minority of radial blood vessels was surrounded by zones up to 50 μm in width of reduced staining, in which predominantly astroglial lamellae were devoid of S100 immunoreactivity. Cell bodies and large processes were less affected than small ones. These staining defects were not evenly distributed in the brain or neocortex, but were preferentially localized in the temporo-parietal cortex including a region around the rhinal sulcus; the defects were most prominent in animals older than 70 days. Perivascular defects were probably not only caused by preferential elution of S100 from perivascular neuropil during perfusion, because immersion fixation also leads to suppression of S100 immunoreactivity in extended parts of perivascular, cortical neuropil.

S100 immunoreactivity was best retained in material which was perfusion fixed with a total aldehyde concentration of 4%–5%. Increasing glutaraldehyde concentrations up to 1% or prolongation of postfixation time progressively reduced immunoreactivity beginning in astroglial lamellae, probably due to increased crosslinking in the tissue and reduced penetration of antibodies. In larger profiles, however, staining remained strong. The antigenicity of S100 was not impaired by postfixation up to 16 h, when 0.3% glutaraldehyde was added or postfixation lasted for 2 h with 1% glutaraldehyde. When the relative concentrations of fixing agents were changed (2.5% glutaraldehyde, 1.5% paraformaldehyde) the total duration of fixation had to be kept below 3 h to maintain at least a low level of stainability.

Suboptimal tissue preparation

Other types of fixation were definitely inferior to the standard method either with the result that the amount of S100 immunoreactivity was lower or the distribution of S100 immunostaining was more uneven. The paraformaldehyde-lysine-periodate fixative and the fixation with carbodiimide reduced astroglial S100 staining, while neuronal S100 labelling remained visible. In freeze-dried and vapour-fixed cryostat sections, the staining intensity was rather low and apparently varied with the fixing agent used (paraformaldehyde>benzoquinone>diethylpyrocarbonate=0). After freeze substitution, the S100 staining was diffusely distributed and even large astrocytic processes had submerged. When precipitation in ammonium sulphate was combined with paraformaldehyde fixation, S100 immunoreactivity was almost completely lost from 20-μm-thick cryostat sections, possibly because aldehydes are not stable under these conditions.

Effects of divalent cations and pH

When the fixative was modified by adding or removing Ca^{++}-, Zn^{++}-ions or by lowering the pH, the S100 immunoreactivity was considerably changed in astroglial processes and lamellae (Table 1, Fig. 3). A moderately low pH (e.g. pH 6.6) suppressed the S100 immunoreactivity in tissue compartments around many large blood vessels (Fig. 3B, E), although there was no apparent loss of staining around small vessels including capillaries. In S100-depleted zones, astrocytes did not appear com-

Table 1 The completeness of immunohistochemical S100 labelling in neocortical astrocytes varies with the fixation conditions. The decrease of immunoreactivity (scored – to – – – –) was evaluated in relation to regions with maximum staining (+). Occasional staining defects are marked (±). Note that maximal loss of immunoreactivity (– – –) resulted in lack of staining of restricted areas of neuropil and was never ubiquitous

Type of fixation	Location of S100 immunoreactivity in astrocytes					
	Lamellae, small processes	Main processes	Perikarya	Overall	Near large blood vessels	Neuropil elsewhere
Perfusion fixation:						
4% paraformaldehyde, 0.3% glutaraldehyde in 0.1 *M* sodium cacodylate						
pH 7.3	±	+	+	+	±	+
pH 6.6	– –	–	–	–	– – –	+
10^{-3} *M* EDTA, pH 7.3	– – –	–	+	+	–	– –
0.1% $CaCl_2$, pH 7.3 ("standard)	±	+	+	++	±	+
10^{-3} *M* $ZnSO_4$, pH 7.3	– –	+	+	+	–	+
0.1 *M* phosphate buffer, pH 7.3	–	+	+	–	+	+
Non-buffered 4% formalin	– –	– –	– –	– –	– – – –	– –
0.5% $ZnCl_2$, pH 5–6						
Immersion fixation:						
4% paraformaldehyde, 0.3% glutaraldehyde in 0.1 *M* sodium-cacodylate						
10^{-2} *M* $CaCl_2$, pH 7.3	–	–	+	+	– –	+
Cryostat sections of fresh frozen brain fixed on slides:						
0.1 *M* sodium cacodylate	– – –	– –	–	– –	– – –	– – –
10^{-2} *M* $CaCl_2$, pH 7.3						

pletely S100-negative and cell bodies at least were labelled. The majority of astrocytes around large blood vessels, however, were partially affected showing weakly stained major processes and no staining of small processes and lamellae. Apparently, there was no preferential loss from processes leading to perivascular endfeet. However, in electron micrographs of neuropil fixed at pH 6.6, many astroglial processes and lamellae were unstained or weakly S100-positive. There were no signs of swelling or destruction of plasma membranes.

When tissue calcium was captured by adding EDTA to fixatives, loss of S100 immunoreactivity was even more dramatic than at low pH, and a different staining pattern appeared (Fig 3C, F). There was no preferential effect on perivascular tissue compartments, rather astrocytic processes were unstained in larger portions of the tissue. Many astrocytes had lost S100 immunoreactivity even from large processes, while other subpopulations of astrocytes were much less influenced (bent arrows in Fig. 3F); the less affected cells were lying isolated or in small clusters. Electron microscopy revealed that in the latter cases horseradish peroxicase-reaction product in stained lamellae and small processes was not restricted by intact plasma membranes. Around some of these labelled structures, reaction product had diffused into neighbouring neuronal components such as axons, dendrites and synapses, which are otherwise unlabelled.

Perfusion fixatives supplemented with EDTA differentially influenced various brain regions. The lateral hypothalamus was devoid of any label. In the hippocampus, astrocytes showed an evenly decreased staining intensity. The neocortical laminae I to V showed a patchy S100 distribution (Fig. 3C). Lamina IV, parts of subcortical white matter and the entire entorhinal cortex were on average less affected. Comparison of S100 immunoreactivity in various brain regions revealed that the cerebellar Bergmann glial cell is apparently the most resistant glial cell type.

Some changes were produced by supplementing the fixative with Zn^{++}-(10^{-3} *M*) or Ca^{2+}-ions (~10^{-2} *M*) at neutral pH. Both kinds of ions enhanced the S100-staining intensity in local neuropil but did not noticeably increase the number of labelled astroglial processes or cell bodies. While the addition of Ca^{2+} resulted in homogeneous staining of large areas of brain tissue, Zn^{2+} slightly increased the number of S100-depleted perivascular spaces at neutral pH. Adding 0.5% $ZnCl_2$ to unbuffered formalin shifted the pH to 5.0–6.0. Perfusion with these solutions produced prominent differences between areas of maximum staining of astrocytes and numerous perivascular aisles of S100 depletion; these effects resembled those of low pH. Otherwise the effects appeared to be rather specific for these divalent cathions, at least in so far as exchanging the buffer substances did not significantly modify the patterns and intensity of staining.

To exclude diffusion artefacts, we studied S100 immunoreactivity in 15-µm thick cryostat sections of unfixed, frozen brain. Mounted, moist sections were either immediately fixed by immersion in 4% paraformaldehyde and 0.3% glutaraldehyde dissolved in 0.1 *M* sodium cacodylate at pH 7.3 or preincubated with 300 µl 0.1 *M* MOPS buffer (~100-times the section volume) for 1 h prior to fixation (Fig. 4). The latter pretreatment was to study effects of S100 elution at different Ca^{2+}-concentrations (Fig. 4B, C, E) and pH (Fig. 4B, D). To estimate possible influences of the redistribution and binding of S100 to tissue compartments, a second set of sections was pretreated with buffers containing S100b at 1 mg/ml

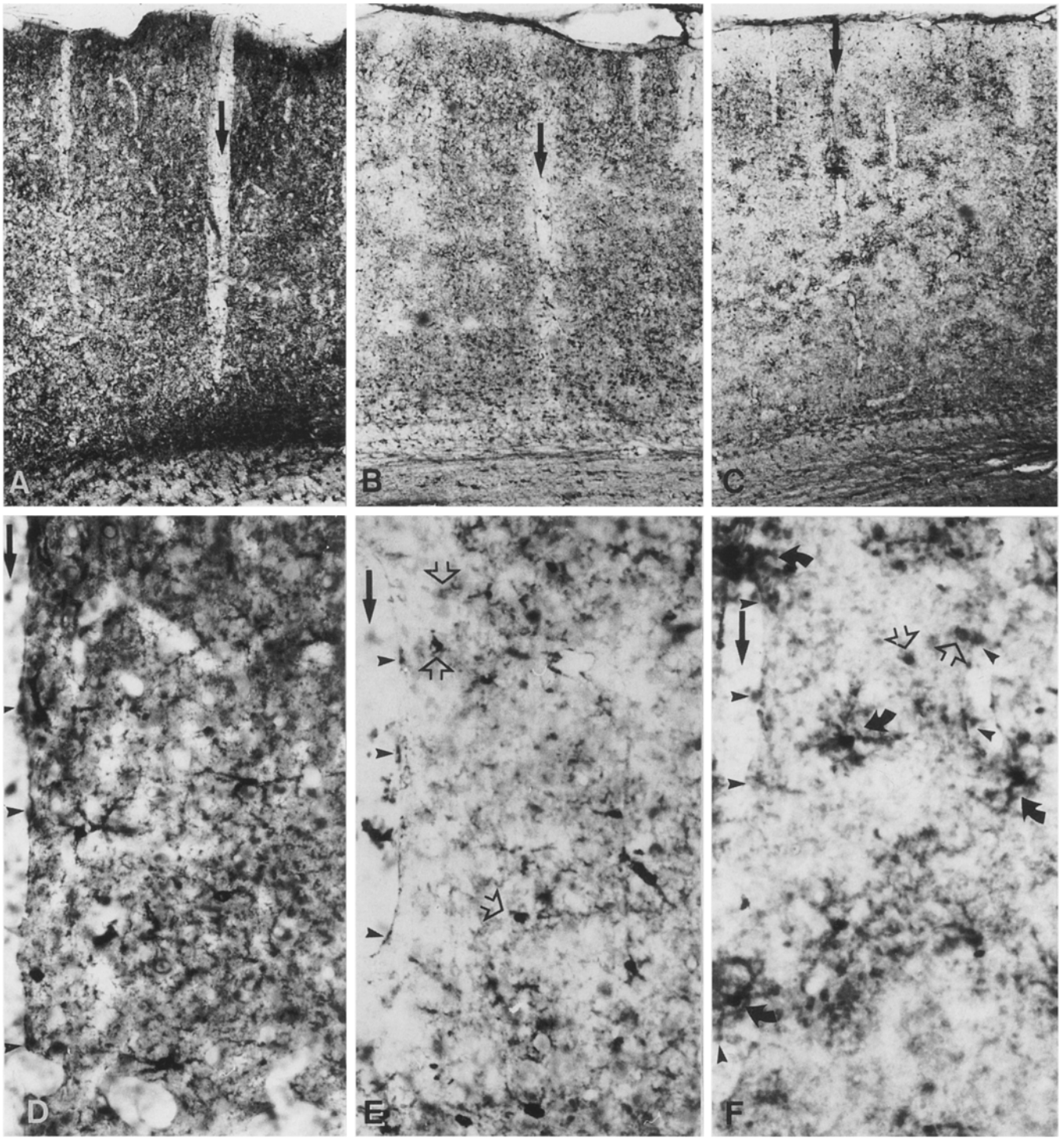

Fig. 3A–F Patterns of S100 immunoreactivity obtained with various types of perfusion fixation in the parietal cortex. **A, D** After standard fixation at pH 7.3, the overall staining intensity is high based on selective staining of astrocytes including their processes. Variation in staining density apparently depend on variations in antibody penetration into the vibratome section. Note, however, that the interior of blood vessels (*arrows*) and neuronal tissue components also exclude staining. **B, E** Fixation at pH 6.6 induces an overall reduction in staining intensity and selective staining defects mainly around large blood vessels. **C, F** Fixative supplemented with 10 m*M* EDTA induces S100 loss which is spatially unrelated to blood vessels. In depleted astrocytes staining is often restricted to perikarya (*open arrows* in **E, F**). Note that some fully stained astrocytes occur even after EDTA-supplemented fixation (*bent arrows* in **F**). **A–F** Radial blood vessels are indicated by *arrows*; vascular endfeet of astrocytes are indicated by *arrowheads*. **A–C** ×58; **D–F** ×270

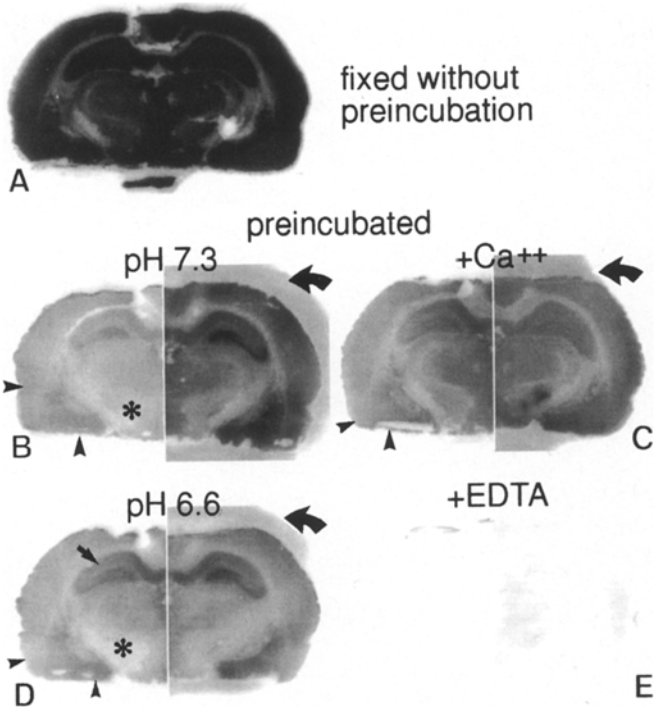

Fig. 4A–E S100 immunoreactivity in 15-μm-thick cryostat sections of unfixed brain. Direct comparison of grey levels is possible, because all sections were simultaneously scanned and generally adjusted for contrast on a computer. **A** The control section shows maximum staining when fixed immediately in 4% paraformaldehyde, 0.3% glutaraldehyde in 0.1 *M* sodium cacodylate at pH 7.3. **B–E** Sections preincubated in supplemented/unsupplemented 0.1 *M* MOPS buffer before fixation, either in buffer alone (*left* halves), or in buffer plus 1 mg/ml bovine S100b (*right*) to check for possible S100 binding. **B**, **C**, **E** The effect of Ca^{2+}-ions is demonstrated at pH 7.3: staining intensity with 10 m*M* Ca^{2+} (**C**) is stronger than without addition of Ca^{2+} (**B**), and no staining is detectable with 10 m*M* EDTA (**E**). **D** Acidic buffer (pH 6.6) without additions. On the left side of **B** to **D**, S100 retention is above average in hippocampus (*arrow*) and entorhinal region (*arrowheads*) and below average in the lateral hypothalamus (*asterisk*). *Bent arrows* indicate strong S100 binding to the activated slide surface. ×2.5

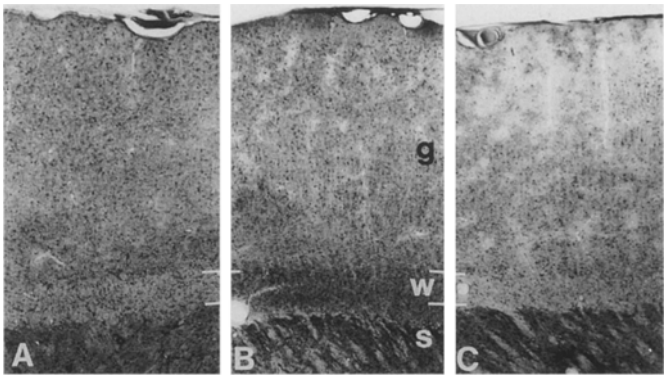

Fig. 5A–C Anaesthesia may induce conditions in which S100 immunoreactivity is reduced in the frontoparietal cortex. **A** Perfusion 7 min after urethane injection allows for homogenous S100 staining. **B** After 1 h of urethane anaesthesia, S100 staining is selectively lost from small zones of neuropil around larger blood vessels. **C** After 1 h barbiturate, perivascular loss is more prominent especially in superficial cortical layers. Note that staining defects are restricted to cortical grey matter (*g*) and are absent from subcortical white matter (*w*) and striatum (*s*). ×17

(right parts of Fig. 4B–E), which is comparable to the S100 concentration in rat brain (Matsutani et al. 1985; Kato et al. 1990).

All pretreated sections showed lower levels of immunoreactivity than the sections that were immediately fixed. At the same time, S100 was bound to the aldehyde activated surface of the microscope slides in the presence of Ca^{2+} (bent arrows in Fig. 4). These experiments demonstrate that in the complete absence of Ca^{2+}, S100 cannot be bound to tissue components and is therefore not fixed by aldehydes. Consistent with this assumption, chelating Ca^{2+} with EDTA resulted in a complete loss of S100 immunoreactivity from both the tissue and the slide surface (Fig. 4E). EDTA prevented fixation of S100 at neutral pH indicating that this effect was a result of calcium loss rather than pH. Ca^{2+}-ions improve fixation of S100 to the tissue. This effect was much clearer in cryostat sections treated with Ca^{2+}-containing solutions than in perfusion fixed brains. In the presence of Ca^{2+} (contained in the tissue), cryostat sections unexpectedly lost more S100 at pH 7.3 than at pH 6.6 though binding of exogenously added S100 seemed slightly higher at pH 7.3 (cf. Fig. 4B and D).

Regional differences in S100 loss from cryostat sectioons became apparent at pH 7.3 and pH 6.6, when only the tissue calcium was present in the incubations. S100 immunoreactivity was very resistant to manipulation in some parts of the hippocampus (CA3,CA4, dentate gyrus) and in the entorhinal cortex. In contrast, S100 immunoreactivity was very dependent on Ca^{2+}-supplementation in other brain regions, especially lateral hypothalamic areas. Ca^{2+}-concentration and pH were effective in changing the S100 distribution "postmortally" in cryostat sections as during perfusion fixation.

Premortal conditions modifying S100 immunoreactivity

Effects of various types of anaesthesia were compared in brains fixed by perfusion with 4% paraformaldehyde, 0.3% glutaraldehyde in 0.1 *M* sodium phosphate buffer, pH 7.3, i.e. in these cases no calcium was added or extracted by chelation. For short duration, deep anaesthesia was maintained for 10 min prior to tissue fixation. Ketavet/Rompun und urethane lead to S100 distribution patterns indistinguishable from those after anaesthesia with ether (Fig. 5A). In contrast, CO_2-induced anesthesia induced narrow, perivascular zones in the neocortex which were S100-negative as early as after 2 min of anaesthesia.

When animals were anaesthetized with pentobarbital or urethane for 1 h the distribution of S100 immunoreactivity was changed. Under these conditions, immunostaining was lost from astrocytes especially in the neocortex. In urethane-anaesthetized brains the S100 deple-

tion was relatively discrete and unstained astrocytes were restricted to the immediate surroundings of large blood vessels (Fig. 5B). After barbiturate, the loss of S100 staining was dramatic and spread over large parts of the neuropil (Fig. 5C). Remarkably, the neocortical grey matter was more affected than other brain regions. The medial and lateral geniculate bodies and the pontine nuclei even showed increased S100 staining in the same section. The pattern of anaesthesia-induced staining defects was similar to that produced by the acidic fixatives (cf. Fig. 5B, C with Fig. 3B).

Discussion

The present results confirm that aldehyde fixatives provide conditions for a reasonably good preservation of S100 immunoreactivity. The standard fixative (4% paraformaldehyde, 0.3% glutaraldehyde in 0.1 *M* sodium-cacodylate, pH 7.3) allowed for more or less even staining of astrocytes in large regions of brain, although occasionally S100-free zones appeared especially in the neocortex. A glutaraldehyde content of ca. 0.3% favourably affected S100 immunoreactivity, especially in cell bodies and major processes, if the fixation time was kept short. This indicates that S100 is effectively crosslinked with the tissue, before the antigenicity begins to deteriorate. However, with increasing fixation time the crosslinking with glutaraldehyde decreased penetration of immunological reagents and thus appeared to suppress the overall staining density as observed at the light microscopic level of resolution.

The supplementation of 0.1% $CaCl_2$ to the standard fixative makes a major difference to fixatives currently used for S100 immunocytochemistry according to reports in the literature (e.g. Cocchia 1981; Van Eldik et al. 1984). Ca^{2+}-ions appeared to support S100 immunoreactivity if added before fixation. Ca^{2+}-addition was most potent in the preincubation medium for cryostat sections of unfixed tissue, while in sections of perfusion fixed brains the increase of the overall staining intensity was moderate. Withdrawal of Ca^{2+} by EDTA resulted in a dramatic decrease of S100 immunoreactivity. Especially affected were astroglial lamellae which make up half of the astroglial cell volume (Wolff 1968), but prolonged EDTA treatment after rupturing of plasma membranes (as in cryostat sections) resulted in complete loss of S100 immunoreactivity. Thus, Ca^{2+}-ions may in some way stabilize the S100 immunoreactivity in brain tissue.

Ca^{2+}-binding changes the conformation of S100 such that a highly reactive sulphydryl group is incovered (Baudier and Cole 1988). It is thought that Ca^{2+}-loaded S100 monomers easily react with other molecules, while they form S100 dimers in the absence of Ca^{2+} (Calissano et al. 1976). S100β can even form oligomers which have a higher disulphide linkage than dimers (Kligman and Marshak 1985). The degree of polymerization may enhance the level of S100 immunoreactivity. In Western blots, antibodies preferably recognized dimeric and oligomeric forms of S100β (Baudier and Cole 1988). Astrocytes of the adult brain seem to contain enough S100 to allow for oligomer formation. In cerebral hemispheres of rat, soluble S100 amounts to 25.8 µg/g wet weight (Matsutani et al. 1985). If 90% of this S100 is localized in astrocytes which provide 9% of the neuropil volume (Rickmann et al. 1990), the concentration of S100 can be estimated to about 250 µg/ml or 12 µ*M* S100 dimer. At these concentrations not only S100 monomers but also S100 dimers were shown to react with τ(2)-proteins in vitro, and the reaction was Ca^{2+}- and pH-dependent (Baudier and Cole 1988). S100 dimers may dissociate as evidenced by the subunit exchange of S100a and S100b at low pH (e.g. pH 2.8) or 1 m*M* Ca^{2+} (Baudier and Gérard 1986).

These biochemical data indicate ample possibilities to explain the Ca^{2+}-dependent retention of S100 immunoreactivity in fixed tissues including direct reactions of aldehydes with sulphydryl groups (Pearse 1980, p. 98). Supplementing fixing solutions with calcium, therefore, can be recommended for S100 immunohistochemistry, e.g. when low concentrations of S100 that are not able to be complexed with tissue components are to be visualized.

On binding of Ca^{2+}-ions, S100 becomes hydrophobic (Calissano et al. 1974; Kligman and Hilt 1988). In this state, S100 may bind to other hydrophobic domains in the tissue as discussed by Moore (1988) and become fixed subsequently; however, Ca^{2+}-dependent hydrophobic interactions have been mainly shown for the α subunit of S100 and not for S100b (Baudier and Gérard 1986), which predominates in the rat brain (Kato et al. 1990). In our electron microscopic preparations, no association between S100 and the apolar core of membranes has been observed. Membrane-bound S100 was apparently not detected by immunohistochemistry after strong fixation with aldehydes, because EDTA-treated cryostat sections were completely unstained after fixation. However, these sections should have contained that fraction of S100 which in vitro remains complexed to membranes in EDTA containing media (Donato 1991). Possibly membrane-bound S100 can be shown after mild, EDTA-supplemented fixation with paraformaldehyde alone (Haglid et al. 1976) which however eliminates most of the cytosolic S100.

In our preparations, inhomogeneity of the S100 distribution was most prominent when tissue calcium was chelated by EDTA during perfusion fixation. On the basis of several lines of evidence, perfusion effects on perivascular neuropil cannot explain the different patterns. Firstly, there were well-perfused brain areas such as the entorhinal region which displayed an even staining of astrocytes. Secondly, even in the most affected neocortical areas, some astrocytes in a direct perivascular location were more or less completely stained. Thirdly, perivascular defects were also seen after immersion fixation. Apparently, there are additional conditions which determine the loss of S100 immunoreactivity when Ca^{2+}-ions are withdrawn from brain tissue. In cultured astrocytes, the

resting concentration of free, intracellular Ca^{2+} is about 50 n*M* (Jensen and Chiu 1990). This concentration is at least two orders of magnitude too low to induce the conformational changes occurring when S100 binds Ca^{2+}-ions with affinities ranging from 10^{-6} to 10^{-3} *M*. Nevertheless, the calcium transients observed after stimulation of glutamate receptors could increase $[Ca^{2+}]_i$ to levels where it can be bound by S100 in the presence of Zn^{2+} and absence of K^+ (Baudier et al. 1986). The successful fixation of S100 in cryostat sections after incubation only in the presence of endogenous calcium indicates that very low Ca^{2+}-levels may be required to keep S100 bound to insoluble tissue components for times long enough for complete fixation by aldehydes. Thus, calcium-dependent variations in S100 immunoreactivity may depict premortal variations in $[Ca^{2+}]_i$ (Jensen and Chiu 1990) of astrocytes and could partly account for the inhomogeneities of astroglial S100 immunoreactivity observed after perfusion with EDTA-supplemented aldehyde fixatives.

Perfusion fixation at pH 6.6 reduced S100 immunoreactivity predominantly in the neocortex and preferentially in a location around large blood vessels. Although in certain glial cells pH may be regulated independently from calcium (Deitmer et al. 1993), we cannot exclude the possibility that the staining defects seen in our specimens were caused by effects of pH on $[Ca^{2+}]$. After fixation at low pH, the S100 distribution was distinctly different from that observed after withdrawal of Ca^{2+}. Since S100-negative areas or aisles were also observed when neocortical tissue was fixed by immersion in the standard fixative, this pattern of defective S100 staining does not depend on perfusion effects. Elution of S100 by the perfusate should have primarily affected the neuropil around capillaries which have a thin endothelium and provide large surfaces for rapid exchange. At present, no remedy can be suggested to counteract the perivascular defects in S100 staining induced by acidic fixatives. Supplement of Zn^{2+} overcomes the overall attenutation of S100 staining in positive structures, but cannot prevent the staining defects around large blood vessels.

Defects of S100 immunoreactivity seen after 1 h urethane anaesthesia showed a very similar distribution pattern to the pattern after perfusion at low pH. This may suggest that animals were suffering from respiratory acidosis. Also the S100-negative zones after 2 min of CO_2 or 1 h of barbiturate anaesthesia may be based on effects of acidosis directly caused by CO_2 or by respiratory suppression in the case of barbiturates. Astrocytes around large blood vessels and in superficial cortical laminae were mainly affected. These neuropil compartments surround the Virchow-Robin spaces, into which S100 may be released. Such a characteristic release site would also explain the occurrence of S100 in the cerebrospinal fluid (Shashoua et al. 1984; Persson et al. 1987).

The data presented show that appropriate tissue preparation starting with anaesthesia that helps to avoid acidosis, is essential for optimal immunohistochemistry of S100 proteins in the brain. At present, presumably there is no way to demonstrate by immunohistochemistry all fractions and molecular forms of S100 simultaneously. However, the procedure of tissue preparation can be optimized up to the level at which changes in the premortal state of neuropil can be detected in fixed tissue by S100 immunoreactivity.

Acknowledgements This work was supported by the German Science Foundation (DFG Wo 279/6). We should like to thank Dr. B.D. Boss for generously supplying the G12B8 antibody. Ms. H. Böttcher, H. Kern, A. Wolff, Mrs. B. Rülke and Mr. R. Dungan gave excellent technical and photographic assistance.

References

Adams JC (1981) Heavy metal intensification of DAB-based HRP reaction product. J Histochem Cytochem 29:775

Baudier J, Cole RD (1988) Reinvestigation of sulfhydryl reactivity in bovine brain S100b ($\beta\beta$) protein and the microtubule-associated τ proteins. Ca^{2+} stimulates disulfide cross-linking between the S100b β-subunit and the microtubule-associated $\tau(2)$ protein. Biochemistry 27:2728–2736

Baudier J, Gérard D (1986) Ions binding to S100 proteins. II. Conformational studies and calcium-included conformational changes in S100 alpha alpha protein: the effect of acidic pH and calcium incubation on subunit exchange in S100a (alpha beta) protein. J Biol Chem 261:8204–8212

Baudier J, Glasser N, Gérard D (1986) Ions binding to S100 proteins. I. Calcium- and zinc-binding properties of bovine brain S100 alpha alpha, S100a (alpha beta), and S100b (beta beta) protein: Zn^{2+} regulates Ca^{2+} binding on S100b protein. J Biol Chem 261:8192–8203

Boyes BE, Kim SU, Lee V, Sung SC (1986) Immunohistochemical colocalization of S-100b and the glial fibrillary acidic protein in rat brain. Neuroscience 17:857–865

Calissano P, Alema S, Fasella P (1974) Interactions of S-100 protein with cations and liposomes. Biochemistry 13:4553–4560

Calissano P, Mercanti D, Levi A (1976) Ca^{2+}, K^+-regulated intramolecular crosslinking of S-100 protein via disulfide bond formation. Eur J Biochem 71:45–52

Cocchia D (1981) Immunocytochemical localization of S-100 protein in the brain of adult rat. Cell Tissue Res 214:529–540

Deitmer JW, Schneider HP, Munsch T (1993) Independent changes of intracellular calcium and pH in identified leech glial cells. Glia 7:299–306

Donato R (1991) Perspectives in S-100 protein biology. Cell Calcium 12:713–726

Donato R, Prestagiovanni B, Zelano G (1986) Identity between cytoplasmic and membrane-bound S-100 proteins purified from bovine and rat brain. J Neurochem 46:1333–1337

Dyck RH, Van Eldik LJ, Cynader MS (1993) Immunohistochemical localization of the S-100 beta protein in postnatal cat visual cortex: spatial and temporal patterns of expression in cortical and subcortical glia. Dev Brain Res 72:181–192

Eng LF, Bigbee JW (1978) Immunochemistry of nervous system-specific antigens. Adv Neurochem 3:43–97

Ghandour MS, Langley OK, Labourdette G, Vincendon G, Gombos G (1981) Specific and artefactual cellular localizations of S100 protein: an astrocyte marker in rat cerebellum. Dev Neurosci 4:66–78

Goto S, Matsukado Y, Uemura S, Mihara Y, Inoue N, Ikeda J, Miyamoto E (1988) A comparative histochemical study of calcineurin and S-100 protein in mammalian and avian brains. Exp Brain Res 69:645–650

Haan E, Boss BD, Cowan WM (1982) Production and characterization of monoclonal antibodies against the "brain specific" proteins 12-3-2 and S-100. Proc Natl Acad Sci USA 79:7585–7589

Haglid KG, Hamberger A, Hansson H-A, Hydén H, Persson L, Rönnbäck L (1976) Cellular and subcellular distribution of the S-100 protein in rabbit and rat central nervous system. J Neurosci Res 2:175–191

Haring JH, Hagan A, Olson J, Rodgers B (1993) Hippocampal serotonin levels influence the expression of S100β detected by immunocytochemistry. Brain Res 631:119–123

Hårdemark H-G, Ericson N, Kotwica Z, Rundström G, Mendel-Hartvig I, Olsson Y, Pahlman S, Persson L (1989) S-100 protein and neuron-specific enolase in CSF after experimental traumatic or focal ischemic brain damage. J Neurosurg 71:727–731

Hsu S-M, Raine L, Fanger H (1981) Use of avidin-biotin-peroxidase complex (ABC) in immunoperoxidase techniques: a comparison between ABC and unlabeled antibody (PAP) procedures. J Histochem Cytochem 29:577–580

Jensen AM, Chiu SY (1990) Fluorescence measurement of changes in intracellular calcium induced by excitatory amino acids in cultured cortical astrocytes. J Neurosci 10:1165–1175

Kato K, Suzuki F, Morishita R, Asano T, Sato T (1990) Selective increase in S-100β protein by aging in rat cerebral cortex. J Neurochem 54:1269–1274

Kendall PA, Polak JM, Pearse AGE (1971) Carbodiimide fixation for immunohistochemistry: observations on the fixation of polypeptide hormones. Experientia 27:1104–1106

Kligman D, Hilt DC (1988) The S100 protein family. Trends Biochem Sci 13:437–443

Kligman D, Marshak DR (1985) Purification and characterization of a neurite extension factor from bovine brain. Proc Natl Acad Sci USA 82:7136–7139

Laskawi R, Rickmann M, Böttcher H, Freier S, Wolff JR (1993) Glial changes in the neocortex of the rat following various types of facial nerve lesion. In: Elsner N, Heisenberg M (eds) Gene – brain – behaviour. Thieme, Stuttgart, p 805

Lewis D, Teyler TJ (1986) Anti-S-100 serum blocks long-term potentiation in the hippocampal slice. Brain Res 383:159–164

Ludwin SK, Kosek JC, Eng LF (1976) The topographical distribution of S-100 and GFA proteins in the adult rat brain: an immunohistochemical study using horseradish peroxidase-labelled antibodies. J Comp Neurol 165:197–208

Matsutani T, Nagayoshi M, Tamaru M, Hirata Y, Kato K (1985) Changes in the levels of neural cell specific proteins in the developing rat brain. Neurochem Res 10:1155–1172

Matus A, Mughal S (1975) Immunohistochemical localisation of S-100 protein in the brain. Nature 258:746–748

McLean IW, Nakane PK (1974) Periodate-lysine-paraformaldehyde fixative. A new fixative for immunoelectron microscopy. J Histochem Cytochem 22:1077–1083

Moore BW (1988) The S-100 protein. In: Marangos PJ, Campbell IC, Cohen RM (eds) Neuronal and glial proteins: structure, function and clinical application. Academic Press, San Diego, pp 137–167

Müller CM, Akhavan AC, Bette M (1993) Possible role of S-100 in glia-neuronal signalling involved in activity-dependent plasticity in the developing mammalian cortex. J Chem Neuroanat 6:215–227

Pearse AGE (1980) Histochemistry. Theoretical and applied, vol I, 4th edn. Churchill Livingstone, Edinburgh

Pearse AGE, Polak JM (1975) Bifunctional reagents as vapour- and liquid-phase fixatives for immunohistochemistry. Histochem J 7:179–186

Persson L, Hårdemark H-G, Gustafsson J, Rundstroem G, Mendel-Hartvig I, Esscher T, Pahlman S (1987) S-100 protein and neuron-specific enolase in cerebrospinal fluid and serum: markers of cell damage in human central nervous system. Stroke 18:911–918

Popov N, Schulzeck S, Pankova TM, Ratushnyak AS, Starostina MV, Shtark MB, Matthies H (1988) Alterations in calmodulin and S-100 protein content of hippocampal slices during long term potentiation. Biomed Biochim Acta 47:189–195

Rapport MM, Laev H, Mabadik S, Graf L (1974) Immunohistochemical appearance of the S100-protein in the developing rat brain. Trans Am Soc Neurochem 5:58

Rickmann M, Wolff JR (1992) Astroglial(?) S100-protein. The dynamics of light and electron microscopic distribution. J Hirnforsch 33:117

Rickmann M, v Fischer-Weikersthal L, Wolff JR (1990) The shape of astrocytes. Verh Anat Ges 83:451–452

Riva A (1974) A simple and rapid staining method for enhancing the contrast of tissues previously treated with uranyl acetate. J Microscopie 19:105–108

Shashoua VE, Hesse GW, Moore BW (1984) Proteins of the brain extracellular fluid: evidence for release of S-100 protein. J Neurochem 42:1536–1541

Tabuchi K, Ohnishi R, Furura T, Nishimoto A (1983) Immunohistochemical localization of S-100 protein in human cerebral and cerebellar cortices. Experientia 39:335–337

Turner RJ (1972) Carbodiimide fixation for electron microscopy and immunoelectron cytochemistry. Experientia 28:368–371

Van Eldik LJ, Ehrenfried B, Jensen RA (1984) Production and characterization of monoclonal antibodies with specificity for the S100 beta polypeptide of brain S100 fractions. Proc Natl Acad Sci USA 81:6034–6038

Venable JH, Coggeshall R (1965) A simplified lead citrate stain for use in electron microscopy. J Cell Biol 25:407–408

Verna A (1983) A simple quick-freezing device for ultrastructure preservation: evaluation by freeze-substitution. Biol Cell 49:95–98

Weetall HH (1970) Storage stability of water-insoluble enzymes covalently coupled to organic and inorganic carriers. Biochim Biophys Acta 212:1–7

Wolff J (1965) Elektronenmikroskopische Untersuchungen über die Struktur und Gestalt von Astrocytenfortsätzen. Z Zellforsch 66:811–828

Wolff J (1968) Die Astroglia im Gewebsverbund des Gehirns. Acta Neuropathol (Berl) Suppl 4:33–39